



Reprinted from



February, 1993

Choosing flow monitors for CEMS applications

A key factor in the selection process is the effect of nonuniform flows on the accuracy of the continuous emissions monitoring system.

John G. Olin, Ph.D.
President and CEO
Sierra Instruments Inc.
Monterey, CA 93940

As a result of the 1990 Clean Air Act Amendments¹, electric power plants must reduce their emissions of sulfur dioxide and nitrous oxides—the primary causes of acid rain. The U.S. Environmental Protection Agency (EPA), in its proposed rules², designates the 111 Phase I fossil-fueled plants (roughly 268 boiler units) that must have continuous emissions monitoring systems (CEMS) installed, certified and operational by November 15, 1993. The EPA also designates the 662 Phase II plants (roughly 2,200 boiler units) that have a January 1, 1995 deadline.

Under the rules, each plant is assigned an SO₂ and NO_x mass emissions allowance in tons per year. One allowance authorizes the emission of one ton (2000 lbm) of SO₂ per year. Plants that exceed their allowances are fined \$2000 for each excess ton per year.

Plants that release less than their annual allowance receive one credit per ton of SO₂. Through an emissions credit trading market, utilities can sell or trade their credits to plants exceeding their allowances. At this writing, the estimated market value of each credit is \$300 to \$500.

Plant operators must monitor SO₂ emissions continuously, recording a data point at least every 15 minutes. Each plant must report the hourly average of SO₂ emissions, and compliance with the annual allowance is determined from the sum of the hourly mass emissions over a year.

To monitor SO₂ mass emissions dw/dt (lbm/h), the operator must monitor both the SO₂ concentration C (lbm/scf) and the mass flow rate Q (scf/h) of the stack gas, because:

$$dw/dt = CQ$$

This means that a flow monitor must now be included in systems that monitor dw/dt . Called continuous emissions monitoring systems (CEMS), these systems consist of:

- A sampling probe,
- Gas analyzers for SO₂ and NO_x,
- Opacity meter and flow monitor,
- Data acquisition and handling system.

The accuracy and reliability of the CEMS is far more critical than conventional emissions instrumentation packages because this system becomes something of a money meter—a meter that determines either the amount of a fine or, hopefully, savings in the bank.

The following will analyze the performance of differential pressure, ultrasonic, and thermal flow monitors in three typical continuous emissions monitoring locations, all of which are characterized by nonuniformities in velocity profile and, in some instances, temperature. To help the plant operator choose the right flow monitor for a given CEMS application, an analysis is presented of the errors in accuracy of the three flow monitors when deployed side by side at the three CEMS locations.

EPA's specifications for flow monitors

The EPA uses performance specs² for CEMS flow monitors and describes three basic instrumental methods:

- Differential pressure (ΔP),
- Ultrasonic (Δt), and
- Thermal (ΔT).

According to the rules, CEMS flow monitors must be located at least 2.0 diameters from an upstream flow disturbance, such as an elbow, expansion, or contraction, and at least 0.5 diameters from a similar downstream disturbance. Meeting this criterion in stack locations is usually easy. However, in the duct work leading to the stack, it is often impossible, and the operator must apply to EPA for a special certification.

All flow monitors must properly span the monthly average flow rate, but this isn't a problem with digital electronics. In addition, all flow monitors must undergo periodic Relative Accuracy Test Audits (RATAs). During these au-

Table 1: EPA's frequency of RATAs

Results of Previous RATA Test		Frequency
Before Jan 1, 2000	After Jan 1, 2000	
±15.0%	±10.0%	Semi-Annual
±10.0%	±7.5%	Annual



ditions, the measured flow rate is compared, using paired tests at different plant loads, with the reference flow rate determined by multipoint traverses of the channel's cross section (as specified in EPA's Method 1³ using the type S pitot tube specified in EPA's Method 2⁴). The relative accuracies required are shown in Table 1.

In addition, the EPA requires a daily electronic drift test, which checks out the entire flow monitoring system, except its primary sensing elements. Some flow monitors also do a daily calibration error test, which checks the flow monitor's active sensing elements. These monitors have more reproducibility than those that do only electronic drift tests. As a result, they are more likely to pass the RATA limits shown in Table 1—reducing the frequency of expensive, risk-bearing RATAs from twice a year to once a year.

One utility tells us that it spends roughly \$40,000 in direct and indirect costs per RATA. Thus, moving from semi-annual to annual RATAs would save that utility some \$40,000 per year.

Neither differential pressure nor most thermal flow monitors offer daily calibration error testing because they can't test their active elements (the multiple sensing ports, in the case of differential pressure devices, and the multiple thermal sensors, in the case of thermal flow monitors). Devices that do provide daily calibration error tests include the thermal flow monitor shown in Fig. 1 and 2, plus most ultrasonic flow monitors.

EPA's specification also requires differential pressure flow monitors to back-purge their probes periodically to prevent clogging of the sensing ports, and thermal flow monitors to provide a means, operated daily, to ensure that the thermal sensors avoid error-causing particulate build-up. All commercial differential pressure flow monitors provide back-purging, and the thermal flow monitor shown in Fig. 2 eliminates errors due to particulate build-up by:

1. Operating each thermal sensor continuously at a high differential temperature above stack temperature, thereby using thermophoretic forces to repel smaller particles and keep them from impacting the sensor's surface;
2. Popping off particulates by applying even higher differential temperatures during a three-minute auto-self-cleaning cycle several times daily, much like a self-cleaning oven.

Principle of operation

Let's now look in more detail at the operation and measurement capabilities of differential pressure, ultrasonic, and thermal flow monitors (Fig. 3).

The differential pressure flow monitor, as shown in Fig. 4, consists of an array of one or more probes located at $z = z_0$. The channel's cross section A is divided into n equal areas, as shown in Fig. 5. Each probe has an upstream bore and a downstream bore. Small ports are drilled along the stagnation line of the upstream bore at locations coinciding with the centroid (x_i, y_i, z_0) of each equal area A/n . One or more ports per probe are drilled in the downstream bore to sense static pressure P . A single differential pressure transmitter is hooked up between the ends of the upstream bores and the ends of the downstream bores. It measures a differential pressure ΔP_{ave} .

All differential pressure flow monitors have secondary flows, as shown in Fig. 4. Secondary flows enter the probe via ports with high free-stream velocities and exit ports

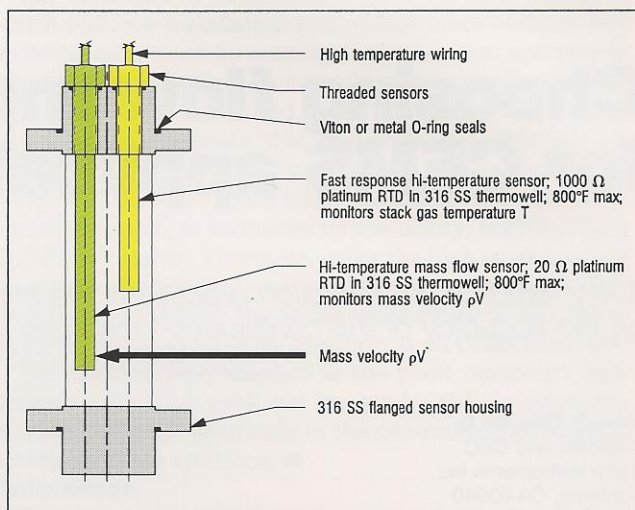


Fig. 1: Thermal monitor has mass flow & temperature sensors.

with lower velocities. The passage of such secondary flows through the ports, as well as wall-friction effects within the upstream bore, all create pressure drops that cause errors in measuring the average velocity.

The net result of all such secondary flows is a total pressure loss that we'll call ΔP_L . Since ΔP_L is proportional to the ratio of the port diameter to the bore diameter raised to the fourth power, the effect of secondary flows is minimized by reducing the diameter of the ports and maximizing the diameter of the bore. However, port diameters can only be reduced so much before clogging by particulates becomes a problem. The measured pressure ΔP_{ave} , therefore, is expressed as:

$$\Delta P_{ave} = \frac{1}{n} \sum_{i=1}^n (P_i - P) - \Delta P_L$$

Ultrasonic flow monitors

The ultrasonic flow monitor (Fig. 6) consists of two ultrasonic transceivers mounted on the channel at angle α (typically 45°, but can range from 6° to 60°) to each other. Multipath configurations, such as one or two "X" patterns, can be deployed to reduce the effect of nonuniform flows.⁵ In operation,⁶ transceiver 1 transmits an ultrasound tone burst (typically 50 kHz) to transceiver 2. Once received by transceiver 2, this unit then sends an identical tone burst back to transceiver 1. The flow monitor measures the transit times t_1 and t_2 , respectively, of the two tone bursts.

To derive Q_{meas} for ultrasonic flow monitors, we must first assume that the velocity V_z and temperature T are uniform, or constant, over the channel's cross section A . Under these assumptions, the speed of sound, a , in the medium is constant, and we can apply the expression:

$$\text{Speed} = \text{Distance/Time}$$

From analysis, we draw the following conclusions:

1. The monitor assumes that the flow velocity and temperature are uniform;
2. The flow velocity is an average along a line path, is not weighted by area or mass, and does not cover the channel's entire cross section;
3. Separate temperature and pressure transmitters are required, thereby compounding the measurement errors.

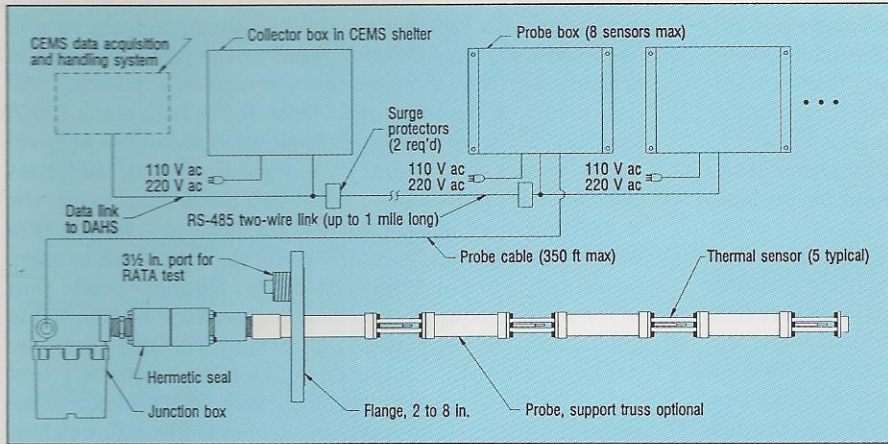


Fig. 2 (left): A complete thermal flow monitor system uses several sensors.

Thermal flow monitors

Figures 1, 2, 5, and 7 describe the principle of operation of thermal flow monitors. The channel's cross section A is divided into n equal areas A/n , similar to that shown in Fig. 5. A typical array consists of four probes—each with five, four, or three thermal sensors—for a total of 20, 16, or 12 points, respectively, all located at $z = z_0$. Each thermal sensor is located at the centroid (x_i, y_i, x_0) of each equal area A/n . The total number of points and the configuration of the equal areas are

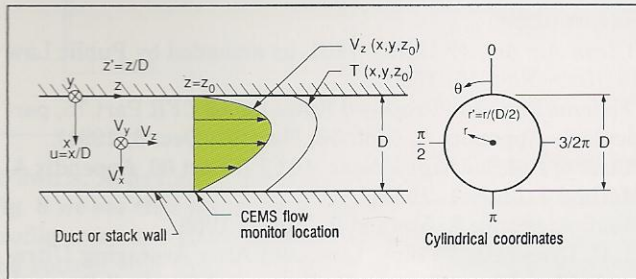
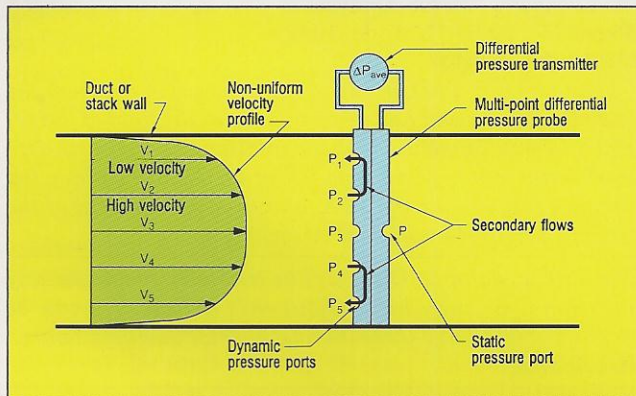


Fig. 3 (above): This is the coordinate system for CEMS monitors. The only velocity component contributing to the net flow rate Q is V_z , which is usually expressed in units of f/s .

Fig. 4 (below): Principle of operation of a differential pressure flow monitor. The device consists of an array of one or more probes—each with an upstream and a downstream bore.



identical to those required by EPA's Method 1: a minimum of 16 points for CEMS monitoring locations between 2 and 6 hydraulic diameters from an upstream disturbance, and 12 points for greater than 6 hydraulic diameters from an upstream disturbance.

All CEMS certification and RATA tests are made at the exact same points in the cross section as the thermal flow monitoring array. The thermal flow monitor shown in Figs. 1 and 2 has a rail system along the side of each probe facilitating repeatable, aerodynamically noninterfering traversal of the type S pitot tube. To reduce the large errors⁷ associated with EPA's Method 2, the type S pitot tube used for RATAs is:

1. Manufactured to close tolerances;
2. Individually calibrated accurately in a wind tunnel;
3. Dedicated specifically to the RATA tests at one plant site;
4. Carefully stored between tests at the plant in an instrument box;
5. Deployed for all RATA tests by the same stack testing team using the same electronic manometer.

Careful attention to the above factors greatly improves the repeatability of the Method 2 tests and, thereby, the passage of RATAs by any flow monitor.

The principle of operation of each thermal sensor is based on the first law of thermodynamics, which states that the electrical power E_v^2/R_v supplied by the electronics to the velocity sensor shown in Fig. 1 is equal to the heat convected away by the flowing stack gas, or

$$E_v^2/R_v = hA(T_v - T)$$

where h is the film coefficient; A is the surface area of the cylindrical sensor; T_v is the temperature of the velocity sensor; and T is the temperature of the stack gas measured by the temperature sensor shown in Fig. 1.

It is the molecules (and hence mass) of the flowing stack gas that interact with the heated boundary layer surrounding the velocity sensor and convect away the heat. Hence, each ther-

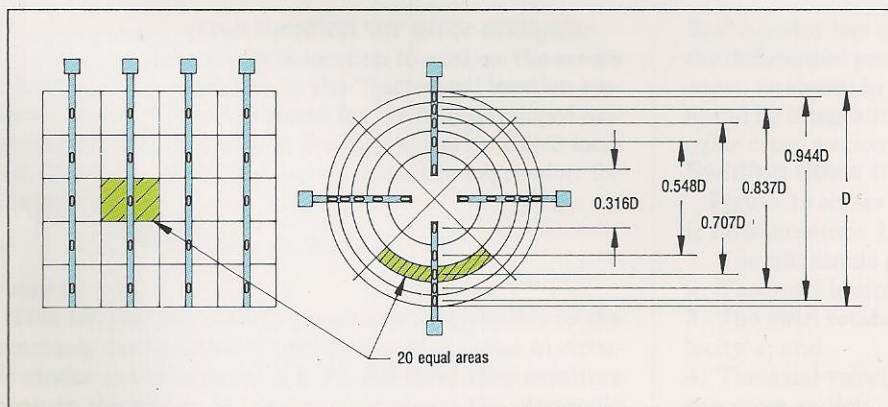


Fig. 5 (left): Typical 20-point arrays in rectangular duct and circular stack for differential pressure and thermal flow monitors. Each array has four probes.

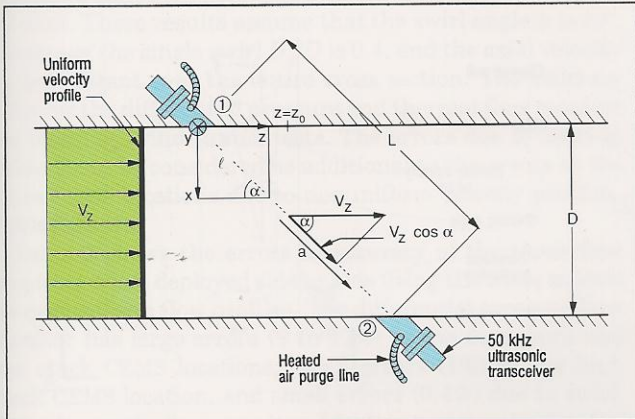
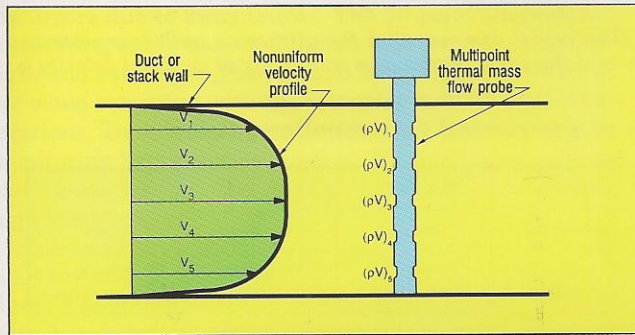


Fig. 6 (above): Principle of operation of an ultrasonic monitor.

Fig. 7 (below): Principle of operation of thermal flow monitors.



mal sensor directly monitors the mass flow rate at the centroid of each equal area in the channel's cross section. The product hA usually is expressed empirically as $hA = a_1 + a_2 (\rho V)^m$, where a_1 , a_2 , and m are empirically determined constants; and ρV is the mass velocity of the stack gas. Solving the equation (above) for the desired quantity ρV we get

$$\rho V = \left[\frac{1}{a_2} \left(\frac{E_v^2 / R_v}{(T_v - T)} \right) - a_1 \right]^{1/m}$$

The electronics shown in Fig. 2 measures E_v^2 / R_v and maintains constant the temperature differential $T_v - T$. Hence, this type of thermal flow monitor is called a constant temperature anemometer, in contrast to another type called a constant current anemometer. The advantage of constant temperature anemometers is that they have fast response to velocity changes (typically 2 s) versus constant current anemometers (typically 60 s). The temperature sensor shown in Fig. 1 responds to stack gas temperature changes in less than 10 s.

The thermal flow monitor in Figs. 1 and 2 does daily calibration error tests by measuring the resistance R_v of the

velocity sensor and the resistance R_t of the temperature sensor. These values are compared with those stored in memory, and a series of additional tests are conducted to insure that the active elements—the velocity and temperature sensors—are in calibration.

The origin of flow nonuniformities

The three most common locations for a CEMS are:

- The rectangular duct work leading to the stack;
- Circular stack at low elevations (3 diameters height, approximately) and;
- Circular stack at high elevations (6 to 10 diameters height, approximately).

As shown in Fig. 8, all three locations are characterized by highly nonuniform velocity profiles, swirling flows, and, in the case of the high and low stack locations with multiple units feeding a single stack, temperature stratifications.

The nonuniform flows shown in Fig. 8 are generated primarily by elbows preceding the CEMS location. The duct work leading to stacks almost always has at least one elbow in the same or different planes. Since the one or more ducts leading to a stack usually are perpendicular to the stack, the high and low stack locations also have upstream elbows. Downstream of the elbows, the momentum of the gas carries most of the stream to the far wall (top wall in Section A-A of Fig. 8), creating a skewed velocity profile. Immediately downstream of an elbow, the velocity gradients are high, and, hence, the viscous forces tending to make the flows uniform are also high. In these instances, the flow is developing and not only varies in the x and y directions, but also in the axial, or z , direction. This will be the case for the duct work and low stack CEMS locations, but not the case for the high stack location, which is nearly fully developed and varies negligibly in the z direction.

Elbows also create secondary flows in the form of vortices

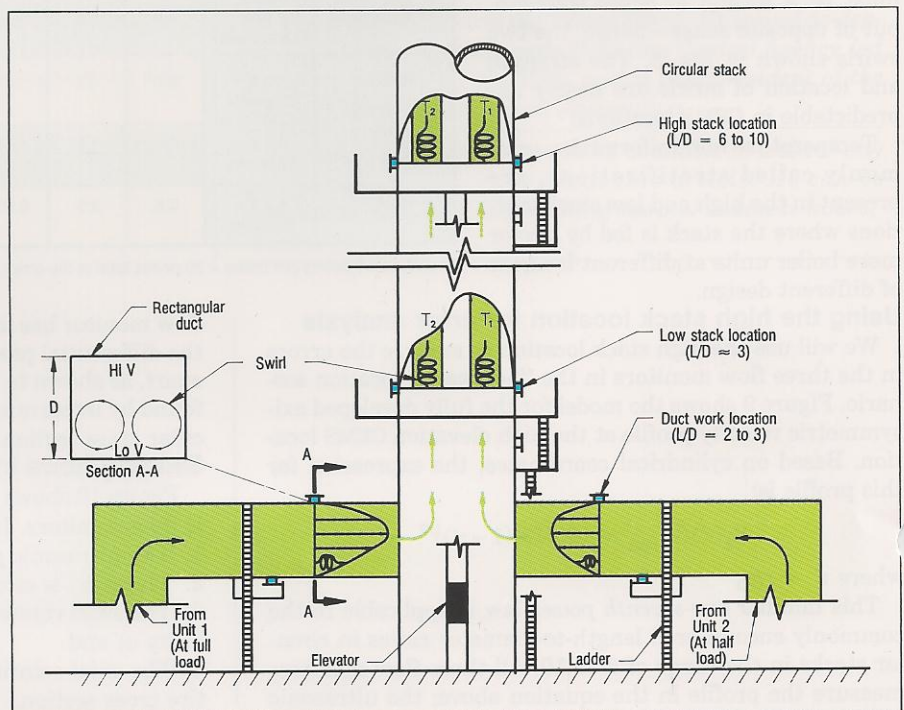


Fig. 8: Non-uniform flows at three common CEMS locations in a power plant.

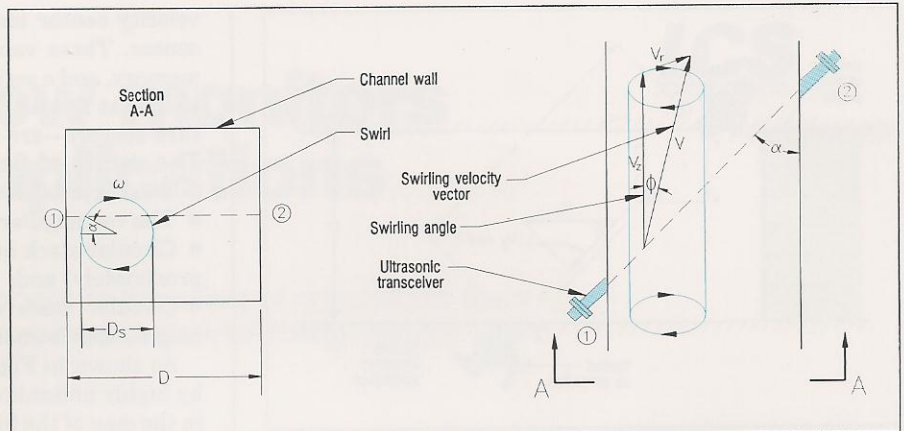
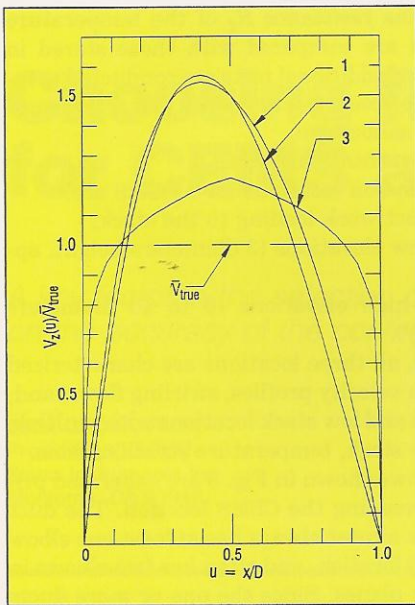


Fig. 9: (left): Three velocity profiles. Curve 1 is the velocity distribution measured by the ultrasonic flow monitor at the duct work and low stack locations. Curve 2 is for reference. Curve 3 is the axisymmetric, fully-developed velocity profile at the high stack location.

Fig. 10 (above): Swirling flow model assumes that the ultrasonic path intersects one swirl; the swirl is circular; and the swirl rotates as a solid body at constant velocity ϕ .

or swirls. Referring to Section A-A of Fig. 8 we see that the skewed velocity profile creates a static pressure near the bottom wall (which has lower velocities) that is higher than the static pressure near the top wall (which has higher velocities). This pressure differential creates a transverse flow from the bottom center to the top center of Section A-A. The containing walls of the channel make this flow close on itself, forming a swirl. The law of conservation of angular momentum says that if there is one swirl, there must be a second of equal strength, but of opposite sense—hence, the two swirls shown in Fig. 8. The strength and location of swirls are nearly unpredictable in CEMS locations.

Temperature nonuniformities, commonly called stratifications, are present in the high and low stack locations where the stack is fed by two or more boiler units at different loads or of different design.

Using the high stack location for error analysis

We will use the high stack location to analyze the errors in the three flow monitors in the “best-case” location scenario. Figure 9 shows the model for the fully developed axisymmetric velocity profile at the high elevation CEMS location. Based on cylindrical coordinates, the expression for this profile is:

$$V_z(r')\bar{V}_{\text{true}} = (60/49)(1-r')^{1/7}$$

where $r' = r/r_0$

This familiar *one-seventh power law* is applicable to the commonly encountered length-to-diameter ratios in circular stacks in the range of 6 to 10. All three flow monitors measure the profile in the equation above; the ultrasonic

Table 2: Flow monitor errors caused by nonuniform flows

CEMS Location:		Duct Work	Low Stack	High Stack	All Locations			
Duct or Stack Cross Section:		Rectangular	Circular	Circular	Both			
Type of Velocity Profile:		Skewed, Developing	Skewed, Developing	Axi-Symmetrical, Fully Developed	Swirl in Uniform Flow			
Type of Flow Monitor	Size of Array	% Error in:						
		$\frac{Q_{\text{meas}}}{Q_{\text{true}}}$	$\frac{Q_{\text{meas}}}{Q_{\text{ref}}}$	$\frac{Q_{\text{meas}}}{Q_{\text{true}}}$	$\frac{Q_{\text{meas}}}{Q_{\text{ref}}}$	$\frac{Q_{\text{meas}}}{Q_{\text{true}}}$	$\frac{Q_{\text{meas}}}{Q_{\text{ref}}}$	$\frac{Q_{\text{meas}}}{Q_{\text{true}}}$
Reference Method	20 points	2.0%	0%	-0.06%	0%	0.6%	0%	—%
Differential Pressure	4 x 5* = 20 points	11.3	9.1	16.4	16.5	1.4	0.8	0.4
Ultrasonic	Two Transceivers	4.9	2.8	39.9	40.0	7.5	6.8	3.5
Thermal	4 x 5 = 20 points	2.0	0	-0.06	0	0.6	0	1.5
	4 x 4 = 16 points	3.1	1.1	-2.4	-2.3	0.7	0.1	—
	4 x 3 = 12 points	5.6	3.5	0.03	0.1	0.9	0.4	—

*4 probes x 5 points per probe = 20 points total in the array.

flow monitor has an angle $\alpha = 45^\circ$; and the four probes for the differential pressure and thermal flow monitors are 90° apart, as shown in Fig. 5. The true average velocity V_{true} is found by integrating the velocity profile over the entire circular cross section.

Swirling flows in ultrasonic flow monitors

Figure 10 shows the model for swirling flows in ultrasonic flow monitors. In this model, we assume:

1. The ultrasonic path intersects only one swirl;
2. The swirl is circular;
3. The swirl rotates as a solid body at constant angular velocity ϕ ; and
4. The axial velocity V_z is constant over the channel's entire cross section.



Table 2 shows the results for swirling flows in a rectangular duct. These results assume that the swirl angle ϕ is 10° , the size of the single swirl D_g/D is 0.4, and the axial velocity V_z is constant over the entire cross section. The swirl results for the differential pressure and thermal flow monitor are based on wind-tunnel tests. The errors due to swirl in Table 2 can be considered as additional to the errors at the three CEMS locations due to nonuniform velocity profiles.

Conclusions

Table 2 shows the errors in accuracy of the three flow monitors when deployed side by side using the three models for nonuniform flow profiles. The differential pressure flow monitor has large errors (9 to 17%) in the duct work and low stack CEMS locations, small errors (1%) in the high stack CEMS location, and small errors (0.4%) due to swirl. The ultrasonic flow monitor has large errors in the low stack location (40%), moderate errors in the duct work location (3 to 5%) and high stack location (7 to 8%), and moderate errors due to swirl (3.5%). The 20-point thermal flow monitoring array has small errors (2.0% max.) at all locations and with swirl. The thermal flow monitor has zero error when compared with the reference method at all CEMS locations. Table 2 also reveals that a 16-point thermal flow monitoring array can be used at the duct work and low stack locations, and the 12-point array can be used at the high stack location.

Since swirling flows are always accompanied by large scale turbulence, the ultrasonic flow monitor will have a reduced signal-to-noise ratio, which can cause additional errors in measuring transit time. It is true that the errors shown in Table 2 are systematic except for swirls, and, therefore, theoretically correctable by applying a bias factor prior to EPA certification. This procedure may be suitable for differential pressure and thermal flow monitors whose arrays provide coverage over the channel's entire cross section. On the other hand, the ultrasonic flow monitor, with its line path coverage, can not sense major alterations in the velocity profile in the remainder of channel resulting from changes in plant load and boiler operating conditions—especially in stacks fed by one or more boiler units. In this case, the bias factor may not be applicable.

The total cost of ownership of all of the flow monitors, which includes installation and maintenance costs as well as initial cost, must be considered by the plant operator in selecting the right flow monitor for a given application. All flow monitors have reduced errors at the high stack CEMS location. Unfortunately, this location is accessible only via an elevator, as shown in Fig. 8, instead of being ladder-accessible like the two lower CEMS locations. As a result, the installation cost, as estimated by one utility, is \$250,000 to \$1,000,000 higher. Therefore, using the high stack location to avoid nonuniform flows is costly. The ultrasonic flow monitor also requires the added expenditure of \$30,000 to \$50,000 for the extra offset platform at all CEMS locations.

The thermal flow monitor is the plant operator's best choice for the duct work and low stack CEMS locations because it performs accurately in the nonuniform flows characterizing these locations. ■

References

- ¹*Clean Air Act*, 42 U.S.C. 7401, as amended by Public Law 101-549 (Nov. 15, 1990).
- ²*Federal Register*, Proposed Rules for 40 CFR Part 75, particularly Appendix A. (Vol. 56, No. 232, Dec. 3, 1991).
- ³*Code of Federal Regulations*, 40 CFR Part 60, Appendix A, Method 1. (July 1, 1988).
- ⁴*Ibid*, Appendix A, Method 2. July 1, 1988.
- ⁵L.C. Lynworth, "Point, Line, and Area Averaging Ultrasonic Flow Measurements in Ducts and Stacks," *Proceedings of the EPRI Heat Rate Improvement Conference*, (November, 1992).
- ⁶Wm. A. Gilmour and D. Stahlschmidt, "Ultrasonic Flow Measurement of Gases for EPA Monitoring," *AWMA* (Paper No. 92-120.07, June 1992).
- ⁷R. L. Myers, "Error-Analysis of EPA Method 2," *AWMA* (Paper No. 92-66.15, June, 1992).

About the author

John G. Olin, PhD, is one of the pioneers in thermal gas flow monitoring and has seven patents in the field of industrial and environmental instrumentation. He served as deputy director for the Minnesota Pollution Control Agency, led research projects for the EPA, and is past president of the Air and Waste Management Association.

The author, John G. Olin, will be available to answer any questions you may have about this article. He can be reached at (800) 866-0200 during normal business hours, Pacific time.